Enhancing Adversarial Robustness of Vision-Language Models through Low-Rank Adaptation

Yuheng Ji*
Institute of Automation, CAS
School of Artificial Intelligence, UCAS

Yue Liu*
Institute of Data Science,
National University of Singapore

Zhicheng Zhang
Institute of Automation, CAS
School of Artificial Intelligence, UCAS

Zhao Zhang
Beijing University of Posts and
Telecommunications

Yuting Zhao
Institute of Automation, CAS
School of Artificial Intelligence, UCAS

Xiaoshuai Hao
Beijing Academy of Artificial
Intelligence

Gang Zhou
Beijing University of Posts and
Telecommunications

Xingwei Zhang
Institute of Automation, CAS

Xiaolong Zheng[†]
Institute of Automation, CAS
School of Artificial Intelligence, UCAS

ABSTRACT

Vision-Language Models (VLMs) play a crucial role in the advancement of Artificial General Intelligence (AGI). As AGI rapidly evolves, addressing security concerns has emerged as one of the most significant challenges for VLMs. In this paper, we present extensive experiments that expose the vulnerabilities of conventional adaptation methods for VLMs, highlighting significant security risks. Moreover, as VLMs grow in size, the application of traditional adversarial adaptation techniques incurs substantial computational costs. To address these issues, we propose a parameter-efficient adversarial adaptation method called **AdvLoRA** based on Low-Rank Adaptation. We investigate and reveal the inherent low-rank properties involved in adversarial adaptation for VLMs. Different from LoRA, we enhance the efficiency and robustness of adversarial adaptation by introducing a novel reparameterization method that leverages parameter clustering and alignment. Additionally, we propose an adaptive parameter update strategy to further bolster robustness. These innovations enable our AdvLoRA to mitigate issues related to model security and resource wastage. Extensive experiments confirm the effectiveness and efficiency of AdvLoRA.

CCS CONCEPTS

• **Computing methodologies → Artificial intelligence**.

KEYWORDS

Adversarial robustness, Low-Rank adaptation, Vision-Language models

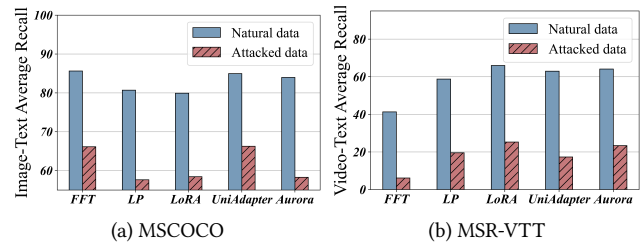* Equal Contribution.
† Corresponding Author.

Figure 1: Vulnerability of vision-language model adaptation methods to natural and adversarial data in MSCOCO (image-text data) [29] and MSR-VTT (video-text data) [60] datasets.

1 INTRODUCTION

Artificial General Intelligence (AGI) aims to create intelligent agents that can perform as well as or better than humans on various cognitive tasks, making it a promising topic for research and industrial applications [17, 45]. As vision and language are key components of intelligence, Vision-Language Models (VLMs) have emerged as a crucial technique for achieving AGI [1, 12].

Recently, the adaptation of VLMs aims to improve the performance on different downstream tasks and has become a hot research topic. However, through extensive experiments, we find the vulnerability of the conventional adaptation methods, e.g., Full Fine-Tuning (FFT) [55, 58, 63], Linear Probe (LP), LoRA [25], Unidapter [36], and Aurora [53] for VLMs, which may bring significant security threats in various domains, such as facial recognition [49, 51], medical analysis [14, 38] and autonomous driving [13, 66]. As shown in Fig. 1, we conduct adaptation experiments of VLMs on the natural and attacked data of the MSCOCO [29] and MSR-VTT [60] datasets. From these experimental results, we find that the average performance drops about 30.98% on the attacked data. To solve
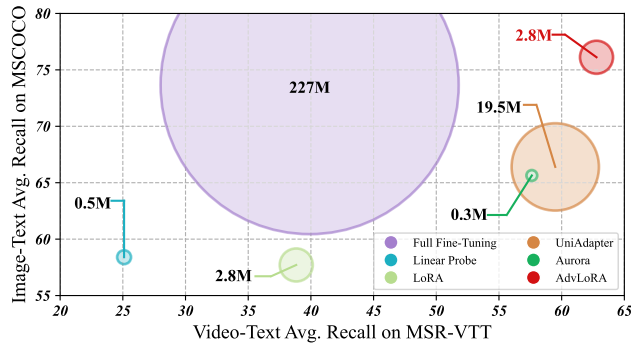
Figure 2: Adversarial robustness and tunable parameter number of adversarial adaptation methods on two dataset.

this problem, various techniques are proposed against adversarial attacks by data augmentation [42, 52], attack detection [30, 41] and adversarial training [18, 31]. As the most effective defense strategy, adversarial training enhances the adversarial robustness of VLMs by retraining the model on mined adversarial examples [39, 44, 50].

However, as the sizes of VLMs increase, the conventional adversarial training method with full parameter updating to improve the adversarial robustness of VLMs will lead to high computing and storage costs [15]. In recent years, Parameter-Efficient Fine-Tuning (PEFT) technology has garnered widespread attention as a novel adaptation paradigm due to its significant success in adapting large-scale pre-trained models. PEFT technologies can adapt VLMs with extremely small additional tunable parameters and achieve comparable or better performance than FFT methods. While PEFT technologies have demonstrated remarkable success in natural scenarios, their application in adversarial attack scenarios remains largely uncharted territory. But simply applying the adversarial training on the conventional adaptation methods will lead to 1) limited defense performance and 2) high computational and storage costs. To verify our points, we visualize the adversarial robustness performance and the tunable parameter number of different adversarial adaptation methods in Fig. 2. From the results, we find that the existing adaptation methods such as FFT and UniAdapter will lead to large parameter costs. Besides, LoRA, LP, and Aurora are not robust to adversarial attacks.

To solve these problems, we aim to develop a parameter-efficient adversarial adaptation method termed AdvLoRA to effectively and efficiently improve the robustness of VLMs against attacks. At first, similar to LoRA, the intrinsic low-rank property of adversarial adaptation for VLMs is revealed. Secondly, we improve LoRA with a novel reparameterizing technology. Concretely, we regard the rank of LoRA as the number of cluster centers and utilize the clustering algorithm to reparameterize LoRA from the weight matrices of VLMs. The weight matrices are decoupled into the clustering centers and the clustering distribution matrices. Subsequently, we impose constraints on their product to align with the parameter distribution of the original weight matrix. Moreover, we design an adaptive parameter update strategy to improve the robustness further. Through these settings, we effectively and efficiently facilitate the adversarial adaptation of VLMs. Our designs on low-rank for adversarial adaptation are motivated by the common dense direction

theory [2], which demonstrates that low-rank adaptation in shallow convolutional neural networks are more suitable to effectively enhance their robustness. For the first time, this paper empirically verifies the applicability of this theory to VLMs and introduces a novel clustering-based initialization method for LoRA, facilitating the process of adversarial fine-tuning. The contributions of this paper are summarized as follows:

- We demonstrate the vulnerability of VLMs with different adaptation methods to adversarial attacks via experiments.
- We investigate and reveal the intrinsic low-rank property during the adversarial adaptation for VLMs.
- We propose a novel parameter-efficient adversarial adaptation method named AdvLoRA with parameter clustering, parameter alignment, and adaptive parameter update.
- We are the first to introduce the adversarial adaptation for VLMs. Extensive experiments demonstrate the effectiveness and efficiency of our proposed method.

2 RELATED WORK

Parameter-efficient Tuning on VLMs. Vision-Language Models (VLMs) excel in various vision-language tasks, such as cross-modal retrieval [19–24] and generation [7, 48]. However, they may struggle when task data diverges from training data, necessitating re-training or fine-tuning on task-specific datasets. Traditional adaptation methods like Full Fine-Tuning (FFT) become inefficient with larger VLMs, prompting the need for parameter-efficient tuning to reduce training and storage costs. Recent approaches inspired by natural language processing [10, 32, 65] and computer vision [5, 26] aim to adapt frozen VLMs using minimal tunable parameters, achieving results comparable to full parameter tuning. These methods fall into three categories: adapter-based [16, 36], prompt-based [37, 59, 70], and LoRA-based [35, 43, 47, 54, 67, 69]. LoRA-based approaches are particularly notable for their reduced tunable parameters, lack of additional input, and minimal inference latency. This paper addresses suboptimal initialization in standard LoRA methods and explores a clustering-based reparameterization strategy to enhance VLM robustness during adaptation.

Adversarial Adaptation on VLMs. Some researchers have shown that artificial neural networks, including Vision-Language Models (VLMs), are vulnerable to unrecognized attacks [8, 33, 34, 68]. Specifically, adding perturbations to inputs can lead VLMs to make incorrect decisions with high confidence. To enhance adversarial robustness, many studies focus on data augmentation [8, 57] and adversarial training [11, 15, 40]. Adversarial training, particularly effective, improves robustness by incorporating adversarial inputs into the training process via a min-max formulation [39]. Initially, some efforts used adversarial training techniques to train VLMs from scratch [15]. Recently, adversarial adaptation has emerged as a cost-effective strategy for enhancing adversarial robustness post-pretraining [40, 61, 62, 64]. However, most methods update all parameters of the pre-trained model and focus on visual models. A few multi-modal approaches, such as TeCoA [40], utilize prompt tuning for adversarial adaptation.

In this paper, we introduce a parameter-efficient LoRA method for adversarial adaptation in cross-modal tasks. Unlike AutoLoRa [61], which updates all parameters while addressing gradient instability,

our approach maintains efficiency. Inspired by dense direction theory [2], which suggests that low-rank adaptation enhances robustness in shallow networks, we provide the first empirical validation of this theory in VLMs and present a novel clustering-based initialization method for LoRA to streamline adversarial fine-tuning.

3 METHOD

In Sec. 3.1, we first define the cross-modal retrieval. Subsequently, addressing the vulnerability of VLMs to adversarial attacks, we introduce an adversarial training module in Sec. 3.2 to enhance the model's adversarial robustness. Finally, to mitigate the high cost associated with adversarial training, we present an adaptation module in Sec. 3.3, which maintains the VLMs' adversarial robustness while reducing the expenses of adversarial training.

3.1 Task Definition

Cross-Modal Retrieval. Cross-modal retrieval aims to utilize information from one modality to retrieve semantically relevant information from another. We select cross-modal retrieval as our benchmark task due to its efficacy in assessing the quality of cross-modal representation learning in VLMs. Under adversarial attacks, cross-modal retrieval serves as an effective metric for evaluating whether models can learn robust feature representations.

Taking image-to-text retrieval as an example, given an image v_i, its semantic representation $z_i^v = \mathcal{F}_v(v_i)$ is used to compute the cosine similarity with each textual representation z_j^w within the text database as follows:

$$\text{sim}(z_i^v, z_j^w) = \frac{z_i^v \cdot z_j^w}{\|z_i^v\| \|z_j^w\|}, \tag{1}$$

where $z_j^w = \mathcal{F}_w(w_j)$ represents the semantic representation derived from the textual data w_j after feature extraction via the text encoder $\mathcal{F}_w$. Then we select the highest similarity text data as the retrieval results. Under adversarial attacked, robust VLMs could learn semantically invariant feature representations so that they will not be misled by small perturbations.

3.2 Adversarial Training Module

Extensive experimentation demonstrated that both VLMs and their variants adapted with PEFT methods are susceptible to adversarial attacks, as illustrated in Fig. 1. Consequently, in this subsection, we design an adversarial training module to enhance the adversarial robustness of VLMs. We begin by introducing the concept of adversarial attacks, followed by the presentation of adversarial training as an effective defense technology for enhancing adversarial robustness.

Adversarial Attack. Adversarial attacks δ is a tensor added to the natural image v, $v_a = v + \delta$, aiming to fool the model into making the incorrect decision as formulated:

$$v_a = \arg\max_{v_a} \mathcal{L}(v_a, w), \quad \text{s.t.} \quad \|v_a - v\|_p \le \varepsilon, \tag{2}$$

where p donates the p-norm, and ε donates the restriction value of values, which is often set to be smaller than $8/255$. Thus, the adversarial attacks are imperceptible to humans. In this paper, we focus on adversarial attacks on visual data, as attacks on natural

language are readily perceptible to humans. Therefore, it is practically significant and more challenging to make attacks on visual data. Concretely, we utilize PGD [39] to generate v_a as follows:

$$v_a = \prod \left\{ \text{clip}_\varepsilon (v + \xi \cdot \text{sign} (\nabla_v \mathcal{L}(v, w))) \right\}, \tag{3}$$

where $\text{sign}(\nabla_v \mathcal{L}(v, w)))$ denotes the sign value of the back-propagated gradient. Besides, ξ is the step size of each iteration. And $\text{clip}_\varepsilon(x) = \min(x, \varepsilon)$ clips each value of x to be smaller than ε and return ε when the value of any dimension exceeds ε. $\prod\{\cdot\}$ denotes the iterative procedure. In this manner, v_a can fool the model to make the incorrect decision. Notably, for video data, we treat it as a collection of images and attack 20% of the frames by randomly sparse sampling [56].

Adversarial Training. Adversarial training technologies refer to retraining the model on attacked data, which can learn semantically invariant features under adversarial attacks. Adversarial training aims to minimize the following objective:

$$\theta = \arg\min_\theta \mathcal{L}(v_a, w), \tag{4}$$

where θ donates the parameters of the model.

3.3 Adaptation Module

Although adversarial training can effectively enhance VLMs' adversarial robustness, it requires updating all parameters based on gradient information, leading to a significant cost overhead. To alleviate this issue, in this subsection, we propose an adaptation module that performs adversarial training on LoRA to reduce the number of tunable parameters, achieving parameter-efficient adversarial adaptation. We first provide a brief introduction to LoRA, followed by the introduction of clustering reparameterization and parameter alignment methods, as well as an adaptive parameter update strategy, to facilitate adversarial adaptation.

LoRA. LoRA achieves parameter-efficient adaptation by updating two low-rank matrices attached to the frozen pre-trained weights. Specifically, given the pre-trained weights $W_0 \in \mathbb{R}^{m \times n}$, and the LoRA matrices $A \in \mathbb{R}^{m \times k}$, $B \in \mathbb{R}^{k \times n}$, the input $X^{(l-1)} \in \mathbb{R}^{b \times m}$ is processed through the following computation to obtain the output $X^{(l)} \in \mathbb{R}^{b \times n}$ as follows:

$$X^{(l)} = X^{(l-1)} W_0 + X^{(l-1)} AB, \tag{5}$$

where $k \ll \min(m, n)$. And A and B are initialized as follows:

$$A \sim \mathcal{N}(0, \sigma^2), \quad B = \mathbf{0}, \tag{6}$$

where $\mathcal{N}$ denotes the Gaussian distribution.

During the adaptation process, W_0 is fixed, while A and B are updated via the gradient descent methods. In our proposed model, AdvLoRA, we freeze W_0 and solely update A, B through adversarial adaptation to achieve adversarial robustness in the model as follows:

$$\theta_{A,B} = \arg\min_{\theta_{A,B}} \mathcal{L}(v_a, w). \tag{7}$$

Our model adheres to conventional practice by incorporating LoRA into both the attention modules and feed-forward networks in BLIP.

Reparameterization and Adaptive Parameter Update. The primary distinction between AdvLoRA and other LoRA-like methods lies in the parameterization process of the matrices A, B. In the original LoRA, a random Gaussian initialization for A and zero

for B, so AB is zero at the beginning of adaptation. In contrast, our model, AdvLoRA, initially performs clustering on the weight matrix W_0 of the pre-trained model, treating the rank k of LoRA as the number of cluster centers. Specifically, given an weight matrix $W \in \mathbb{R}^{m \times n}$ and the rank k, we first randomly initialize k cluster center $C = \{c_1, c_2, \ldots, c_k\}$. Then, for each column w_i of W, compute the distances to each cluster center c_j and assign w_i to the closest cluster as follows:

$$\text{cluster}_i = \arg\min_j \|w_i - c_j\|_2. \tag{8}$$

Then update the cluster centers by computing the mean of all data points assigned to each cluster as follows:

$$c_j = \frac{1}{|S_j|} \sum_{w_i \in S_j} w_i, \tag{9}$$

where S_j is the set of columns of W assigned to cluster j. Repeat the above steps until the cluster centers no longer change significantly or a maximum number of iterations is reached. In this manner, we obtain the cluster center embeddings $C \in \mathbb{R}^{k \times n}$ and the distance assignment matrix $D \in \mathbb{R}^{m \times k}$, where each element d_{ij} represents the distance between the w_i and cluster center c_j. The distance assignment matrix D can be computed using the following formula:

$$d_{ij} = \|w_i - c_j\|_2. \tag{10}$$

And the cluster center representation matrix C is simply the matrix of cluster centers as follows:

$$C = [c_1, c_2, \ldots, c_k]. \tag{11}$$

After the parameter clustering, the clustering assignment matrix $D \in \mathbb{R}^{m \times k}$ and the parameter center $C \in \mathbb{R}^{k \times n}$ can be represented the $A \in \mathbb{R}^{m \times k}$ and $B \in \mathbb{R}^{k \times n}$ in the original LoRA method. By these settings, we provide a better reparameterization of the tunable parameters in LoRA. It separates the parameters into different clusters, which have different functions in the whole network.

After obtaining the matrices A and B, we further impose constraints on their product AB to align with the parameter distribution of the original weight matrix W_0 as follows:

$$\min \|W_0 - AB\|_2. \tag{12}$$

In this manner, we can ensure the initialization of AB is close to W_0 at the beginning of the training.

During the process of model adversarial adaptation, we design an adaptive update parameter, α, to facilitate the model's adaptive learning of robust semantic representations as follows:

$$Y = XW_0 + \alpha \cdot XAB. \tag{13}$$

α is a tunable neural network parameter, which can control the adaptation rate during the adversarial adaptation. In summary, we delineate the entire workflow of AdvLoRA in Algorithm 1.

4 EXPERIMENT

4.1 Experimental Setup

Datasets. We conducted a comprehensive evaluation of our proposed model, AdvLoRA, across two types of retrieval tasks and four widely used datasets. This evaluation highlights AdvLoRA's superior performance in cross-modal understanding tasks, specifically

---

Algorithm 1 AdvLoRA WorkFlow on VLMs.

Require: Images: $V = \{v_1, v_2, \ldots, v_n\}$; Texts: $W = \{w_1, w_2, \ldots, w_n\}$; Visual encoder: $\mathcal{F}_v$; Textual encoder: $\mathcal{F}_w$; Pre-trained weight matrix: W_0; LoRA matrix: A, B; Adaptive parameter: α; Restriction value: ϵ; PGD step: ξ; Loss function: $\mathcal{L}$.
Ensure: Representations of V and W: $Z^v = \{z_1^v, z_2^v, \ldots, z_n^v\}$, $Z^w = \{z_1^w, z_2^w, \ldots, z_n^w\}$.
1: **while** at adversarial fine-tuning stage **do**
2:     Perform clustering algorithm on W_0 and obtain cluster center representation in Eq. (8) and Eq. (9);
3:     Obtain the LoRA matrix A, B from cluster center representation and W_0 in Eq. (10) and Eq. (11);
4:     Impose constraints on A and B with SGD algorithm in Eq. (12);
5:     Calculate the loss l using V, W, Y, $\mathcal{F}_v$, $\mathcal{F}_w$, and the loss function $\mathcal{L}$ in Eq. (5).
6:     Obtain the adversarial attack δ with V, ϵ, k, ξ and l in Eq. (3).
7:     Add δ to original images V to obtain the attacked images V_a.
8:     Update A, B via Eq. (4).
9: **end while**
10: Generate robust representations of V and W to downstream tasks with adversarially adapted A, B and $\mathcal{F}_v$, $\mathcal{F}_w$.

---

image-text retrieval with Flickr30K [46] and MSCOCO [29], as well as video-text retrieval with DiDeMo [4] and MSRVTT [60].

- **Flickr30K** [46] contains 31,783 images and 158,915 captions totally. Each image is often annotated with 5 captions. Following the split in Uniadapter [36] and Aurora [53], we use 1,000 images for testing, another 1,000 for validation, and the rest for training.
- **MSCOCO** [29] is a large dataset containing 123,287 images and 616,435 captions. Each image is annotated with 5 captions. Following the split in Uniadapter [36] and Aurora [53], we use 5,000 images for testing, another 5,000 for validation, and the rest for training.
- **Didemo** [4] contains 10,000 videos and 40,000 annotations. Following Frozen in Time [6], we concatenate all descriptions corresponding to the same video into a single sentence to conduct actually video-paragraphto retrieval task.
- **MSR-VTT** [60] is a popular video-text dataset. It contains 10,000 video and 200,000 captions. Following the split in Uniadapter [36] and Aurora [53], we use 1,000 videos for testing, another 9,000 for training.

Baselines. We compare AdvLoRA with conventional adaptation methods, which are implemented by BLIP: full fine-tuning (BLIP-FFT), linear probe (BLIP-LP); as well as the PEFT method on BLIP: LoRA(BLIP-LoRA), Aurora, and Uniadapter.

- **BLIP-FFT** [28] is a conventional adaptation technique that enhances the performance of BLIP for specific downstream tasks by retraining and updating full parameters in downstream tasks.
- **BLIP-LP** [28] is an adaptation technique that involves adding and training a linear layer on top of the frozen pre-trained model BLIP to adapt to specific tasks.
- **BLIP-LoRA** [25] is a PEFT technology that adapts BLIP by introducing low-rank adapters to capture task-specific information, allowing for efficient adaptation to downstream tasks with minimal tunable parameter updates.

Table 1: Hyperparameter setting

config	Image-text Retrieval		Video-text Retrieval	
	Flickr30K	MSCOCO	Didemo	MSR-VTT
optimizer	AdamW	AdamW	AdamW	AdamW
lr	1e-5	1e-5	1e-4	1e-4
schedule	cosine decay	cosine decay	cosine decay	cosine decay
training bs	16	16	8	8
inference bs	32	32	8	8
frames	-	-	16	16
attack ratio	-	-	20%	20%
epochs	5	5	5	5
training input	384	384	8*224	8*224
inference input	384	384	16*224	16*224
attack type	PGD-3	PGD-3	PGD-3	PGD-3
attack alpha	1/255	1/255	1/255	1/255
PGD-epsilon	1/255	1/255	1/255	1/255
rank	10	10	10	10
adaptive weight	1e-3	1e-3	1e-3	1e-3
weight norm lr	1e-3	1e-3	1e-3	1e-3

- **Uniadapter** [36] is the first adapter-based PEFT technology for parameter-efficient cross-modal adaptation.
- **Aurora** [53] is a parameter-efficient cross-modal transfer learning framework that uses mode approximation to generate a minimal set of tunable parameters, achieving lightweight multi-modal adaptation.

Metrics. We employ *Recall@k* as our evaluation metric, measuring the proportion of relevant items retrieved within the top k results. A higher *Recall@k* indicates better performance in retrieving relevant items, reflecting the model's effectiveness and reliability in information retrieval tasks.

Implementations. Our implementation is based on Salesforce's open-source codebase [28]. Following [36, 53], we also apply BLIP [28] as our vision-language backbone for all tasks. We use PyTorch to implement all experiments on the NVIDIA V100 GPU (32GB). We employ PGD-3 [39] for adversarial adaptation and to assess the model's robustness. For the video-text retrieval task, we follow the work of Wei et al. [56] by adopting an attack strategy that sparsely samples 20% of the video frames. Furthermore, we adopt the setup of BLIP, utilizing a momentum encoder to enhance the retrieval performance of our model. To ensure a fair comparison, the momentum encoder is also applied to the other baseline methods. During the fine-tuning process, the parameters of the backbone model are kept frozen. We present the hyperparameter setting in Tab. 1.

4.2 Performance Comparisons

We compare our method with five baselines across two cross-modal retrieval tasks using four datasets. Specifically, we perform adversarial adaptation based on the PGD-3 attack for all methods and evaluate their performance under adversarial conditions.

Evaluation on Image-Text Retrieval. We conducted experiments on adversarially attacked data for both MSCOCO and Flickr30K, as presented in Tab.2 and Tab.3. The results lead us to two key conclusions: (1) *Performance Under Adversarial Attacks.* After adaptation, AdvLoRA outperforms all other baselines when confronted with adversarial attacks. On MSCOCO, AdvLoRA surpasses other PEFT methods by 12.17% and exceeds FFT by 2.47%, using approximately 100 times fewer tunable parameters. (2) *Enhanced Robustness with Larger Datasets.* AdvLoRA shows improved robustness

on larger datasets, highlighting the potential of PEFT methods to bolster model resilience. On the smaller Flickr30K dataset, the performance of various baselines post-adaptation remains comparable, with no significant robustness increase. However, on MSCOCO, FFT achieves notable robustness but still trails behind AdvLoRA. These results emphasize AdvLoRA's advantages in clustering reparameterization and parameter alignment.

Evaluation on Video-Text Retrieval. We conducted experiments on adversarially attacked data for both DiDeMo and MSR-VTT, as presented in Tab.6 and Tab.7. Our findings lead to the following conclusions: (1) *Adversarial Robustness of AdvLoRA.* AdvLoRA demonstrates excellent adversarial robustness on video data, surpassing all other baselines. In DiDeMo, AdvLoRA slightly outperforms UniAdapter while utilizing seven times fewer parameters. On MSR-VTT, AdvLoRA enhances the model's adversarial robustness by 39.16%, significantly exceeding other baselines. (2) *Improved Robustness with Larger Datasets.* AdvLoRA shows better adversarial robustness on larger datasets. On the smaller DiDeMo dataset, the performance of various baselines after adversarial adaptation remains comparable, with minimal improvements in robustness. In contrast, on the larger MSR-VTT dataset, while UniAdapter achieves notable adversarial robustness, it still falls short of AdvLoRA's performance, using seven times more parameters. These results can be attributed to AdvLoRA's design, particularly in terms of clustering reparameterization and parameter alignment. These results further highlight the design advantages of AdvLoRA in clustering reparameterization and parameter alignment.

4.3 Ablation Study

Effect of Proposed Module. To demonstrate the effectiveness of the proposed module, we conduct an ablation study on the components of AdvLoRA using the Didemo dataset and summarize our results in Tab. 4. Firstly, we explored the impact of the parameter clustering technique. Our experiments, comparing model variant (a) with the baseline, indicate a notable improvement when leveraging knowledge from pre-trained models through parameter clustering. Moreover, the performance gains observed in model variants (a), (b), and (c) highlight that incorporating parameter alignment and adaptive parameter update methods on top of parameter clustering significantly enhances the adversarial adaptability of VLMs. Finally, using all the proposed methods together, i.e. AdvLoRA, results in the best overall performance, achieving a mean recall of 58.01.

Sensitivity Analysis of Rank Size. To demonstrate the impact of different rank sizes on AdvLoRA, we trained a series of models with varying ranks on Flickr30K. The results are shown in Fig. 3. We find that as the rank size increases, the number of tunable parameters increases, but AdvLoRA's performance remains stable, while computational cost rises. Therefore, during adversarial adaptation, performance is not sensitive to rank size, allowing us to choose a smaller rank without significant loss in performance.

Loss Convergence Analysis. To explore the effectiveness of the proposed method in terms of loss convergence, we examine two model variants, LoRA and AdvLoRA, on the Flickr30K dataset. The results are presented in Fig. 4. The experimental findings indicate that (1) AdvLoRA achieves a lower loss early in the training process, demonstrating that techniques we proposed such as parameter clustering can serve as an effective "warm-up," helping VLMs

Table 2: Adversarial experiment on MSCOCO. An asterisk (*) indicates that adversarial adaptation has been performed. The best results are displayed in bold, while the second-best results are underlined.

Method	Tunable Para.	MSCOCO TR				MSCOCO IR				Mean
		R@1	R@5	R@10	R@Mean	R@1	R@5	R@10	R@Mean	
BLIP+FFT+Att	223M	53.38	75.12	82.62	70.37	42.25	67.03	76.47	61.92	66.15
BLIP+FFT*+Att	223M	65.42	84.68	89.4	79.83	47.62	73.43	81.35	67.47	73.65
BLIP+LoRA+Att	2.8M	43.2	66.2	74.8	61.4	35.85	60.4	70.16	55.47	58.44
BLIP+LoRA*+Att	2.8M	42.22	66.12	74.7	61.01	34.69	59.39	69.14	54.41	57.71
BLIP+LP+Att	0.5M	43.22	65.82	74.46	61.17	34.6	58.59	68.86	54.12	57.61
BLIP+LP*+Att	0.5M	44.14	67.18	76.04	62.45	34.57	59.14	69.3	54.34	58.40
UniAdapter+Att	19.5M	53.98	75.66	82.74	70.79	42.02	66.8	76.39	61.74	66.27
UniAdapter*+Att	19.5M	50.76	76.68	85.4	70.95	39.9	67.8	77.88	61.86	66.40
Aurora+Att	0.3M	44.56	67.04	75	62.2	34.98	59.34	68.75	54.36	58.28
Aurora*+Att	0.3M	54.56	77.68	84.52	72.25	40.08	60.17	75.66	60.17	65.64
AdvLoRA+Att	2.8M	46.76	69.18	76.72	64.22	37	61.25	70.76	56.34	60.28
AdvLoRA*+Att	2.8M	**67.28**	**87.16**	**92.76**	**82.4**	**49.02**	**75.88**	**84.59**	**69.83**	**76.12**

Table 3: Adversarial experiment on Flickr30K. An asterisk (*) indicates that adversarial adaptation has been performed. The best results are displayed in bold, while the second-best results are underlined.

Method	Tunable Para.	Flickr30K TR				Flickr30K IR				Mean
		R@1	R@5	R@10	R@Mean	R@1	R@5	R@10	R@Mean	
BLIP+FFT+Att	223M	21.1	38.4	46	35.16	21.96	42.62	51.18	38.58	36.87
BLIP+FFT*+Att	223M	64.6	84.8	87.7	79.03	55.06	79.52	84.46	73.01	76.02
BLIP+LoRA+Att	2.8M	67	81.8	84.2	77.67	58.5	77.48	82.7	72.89	75.28
BLIP+LoRA*+Att	2.8M	65.6	**87.1**	89.5	80.4	54.62	79.92	85.18	73.24	76.82
BLIP+LP+Att	0.5M	55.9	76	81.7	71.2	49.3	70.82	77.48	65.87	68.53
BLIP+LP*+Att	0.5M	56.1	75.7	82.7	71.5	48.14	70.5	78.18	65.61	68.55
UniAdapter+Att	19.5M	67.2	82.5	86.5	78.73	58.26	77.26	83.3	72.94	75.84
UniAdapter*+Att	19.5M	**71.2**	85.8	88.2	81.73	**59.12**	**80.4**	85.82	**75.11**	78.42
Aurora+Att	0.3M	65.4	80.7	84.4	76.83	56.98	76.64	82.22	71.95	74.39
Aurora*+Att	0.3M	69.1	84.1	87.3	80.17	56.8	78.82	83.76	73.13	77.15
AdvLoRA+Att	2.8M	66.2	82.5	85.8	78.17	57.7	77.52	83.32	72.85	75.51
AdvLoRA*+Att	2.8M	71	86.8	**90.7**	**82.83**	58.02	80.1	**85.9**	74.67	**78.75**

Table 4: Ablation study on AdvLoRA components. PC, PA, and PU denote parameter clustering, parameter alignment, and adaptive parameter update, respectively. The metrics TR@Mean and VR@Mean denote the mean recall for text-to-video and video-to-text tasks, respectively, while R@Mean represents the average of TR@Mean and VR@Mean.

Setting	PC	PA	PU	TR@Mean	VR@Mean	R@Mean
Baseline	✗	✗	✗	54.37	54.07	54.22
a	✓	✗	✗	55.36	56.29	55.83
b	✓	✓	✗	**57.85**	57.21	57.53
c	✓	✓	✓	57.69	**58.42**	**58.01**
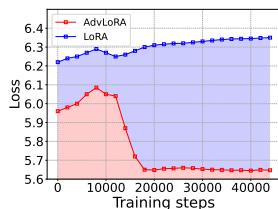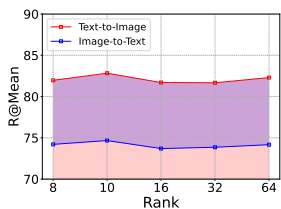
Figure 3: Sensitivity Analysis.   **Figure 4: Loss Analysis.**

Table 5: Comparison on the training time and GPU memory.

Method	Tuable Para.	Time	Mem.
BLIP+FFT	223M	1.00	1.00
BLIP+LoRA	2.8M	0.91	0.85
BLIP+LP	0.5M	0.79	0.67
Uniadapter	19.5M	0.93	0.77
Aurora	0.3M	1.05	1.04
AdvLoRA	2.8M	0.94	0.85

more effective gradient descent trajectory, leading to more efficient model training. In contrast, LoRA appears to get trapped in a local optimum. This highlights the superiority of our proposed method in facilitating better convergence of VLMs.

Efficiency and Storage Cost Analysis. To investigate the cost-effectiveness of the proposed method, we analyze the relative training GPU hours and GPU memory costs of AdvLoRA compared to five baseline models on Flickr30K. The results are presented in Tab. 5, where the time (or memory) of FFT is normalized to one unit. The findings indicate that: (1) AdvLoRA exhibits relatively low parameter count and memory overhead; (2) AdvLoRA incurs longer time costs due to the necessity of offline clustering reparameterization and parameter alignment prior to adaptation.

Performance on More Attacks. To demonstrate the robust generalization of the proposed method, we apply additional attacks

establish a favorable starting point during adversarial adaptation; (2) as training progresses, AdvLoRA successfully navigates to a

Table 6: Adversarial experiment on MSR-VTT. An asterisk (*) indicates that adversarial adaptation has been performed. The best results are displayed in bold, while the second-best results are underlined.

Method	Tunable Para.	MSR-VTT TR				MSR-VTT VR				Mean
		R@1	R@5	R@10	R@Mean	R@1	R@5	R@10	R@Mean	
BLIP+FFT+Att	223M	1.2	5	7.6	4.6	2.7	8.1	12.5	7.77	6.18
BLIP+FFT*+Att	223M	21	41.9	50.8	37.9	21	46.8	57.9	41.9	39.9
BLIP+LoRA+Att	2.8M	12.8	23.4	28.1	21.43	18.9	30.8	37.8	29.16	25.30
BLIP+LoRA*+Att	2.8M	21.2	43.5	52.7	39.13	21	42.5	52.1	38.53	38.83
BLIP+LP+Att	0.5M	7.7	16.1	20.1	14.63	14.4	26.4	32.8	24.53	19.58
BLIP+LP*+Att	0.5M	14.5	26.8	33.3	24.87	15.8	26.7	33.5	25.33	25.10
UniAdapter+Att	19.5M	8.3	15.4	18.9	14.2	11.6	22.6	27.2	20.47	17.33
UniAdapter*+Att	19.5M	<u>38.6</u>	<u>64</u>	<u>74.5</u>	<u>59.03</u>	<u>39.2</u>	<u>64.9</u>	<u>75.8</u>	<u>59.97</u>	<u>59.50</u>
Aurora+Att	0.6M	11.6	20.3	24.6	18.83	16.9	30.1	36.7	27.9	23.37
Aurora*+Att	0.6M	38.1	63.6	73.5	58.4	37	60.8	72.7	56.83	57.62
AdvLoRA+Att	2.8M	12.3	21.8	26.2	20.1	15.8	28.4	34.2	26.13	23.12
AdvLoRA*+Att	2.8M	**40.4**	**67.4**	**78.6**	**62.13**	**40.5**	**68.4**	**78.4**	**62.43**	**62.28**

Table 7: Adversarial experiment on Didemo. An asterisk (*) indicates that adversarial adaptation has been performed. The best results are displayed in bold, while the second-best results are underlined.

Method	Tunable Para.	Didemo TR				Didemo VR				Mean
		R@1	R@5	R@10	R@Mean	R@1	R@5	R@10	R@Mean	
BLIP+FFT+Att	223M	12.66	26.32	35.39	24.79	14.56	31.7	40.58	28.95	26.87
BLIP+FFT*+Att	223M	29.71	53.04	64.3	49.08	31.21	55.63	67.4	51.41	50.25
BLIP+LoRA+Att	2.8M	33.2	57.43	66.7	52.44	32.7	56.73	68.1	52.51	52.48
BLIP+LoRA*+Att	2.8M	33.7	59.82	69.59	54.37	32.8	59.02	70.39	54.07	54.22
BLIP+LP+Att	0.5M	23.13	45.86	53.54	40.84	26.02	47.06	57.03	43.37	42.11
BLIP+LP*+Att	0.5M	22.73	45.46	54.04	40.74	25.32	46.46	56.73	42.84	41.79
UniAdapter+Att	19.5M	27.02	52.14	64.01	47.72	9.27	24.83	36.69	23.6	35.66
UniAdapter*+Att	19.5M	<u>36.38</u>	<u>63.5</u>	**73.57**	<u>57.82</u>	35.88	**64.3**	**73.87**	**58.02**	<u>57.92</u>
Aurora+Att	0.6M	30.31	52.94	64.11	49.12	31.21	54.74	64.61	50.19	49.65
Aurora*+Att	0.6M	35.59	61.22	72.18	56.33	<u>36.69</u>	62.01	71.88	56.86	56.60
AdvLoRA+Att	2.8M	34.4	62.11	71.39	55.97	35.19	62.81	70.99	56.33	56.15
AdvLoRA*+Att	2.8M	**37.38**	**64.4**	<u>73.48</u>	**58.42**	**36.99**	<u>63.21</u>	<u>72.88</u>	<u>57.69</u>	**58.06**

Table 8: Additional attack types on the MSCOCO dataset. "TR" and "IR" donate text-to-image retrieval and image-to-text retrieval.

Method	Attack	TR@Mean	IR@Mean	Mean
LoRA	PGD-3	61.01	54.41	57.71
AdvLoRA	PGD-3	82.40	69.83	76.12
AdvLoRA	PGD-20	81.65	69.13	75.39
AdvLoRA	FGSM	84.44	72.21	78.32
AdvLoRA	BIM	83.25	69.56	76.41
AdvLoRA	SA	87.40	75.83	81.62
AdvLoRA	ZOO	84.17	73.83	79.00

to the AdvLoRA model, which has undergone adversarial adaptation on the MSCOCO dataset. These include white-box attack methods (FSGM [18], PGD-20 [39], BIM [27]) and black-box methods (Zeroth Order Optimization (ZOO) [9], SquareAttack with 500 queries (SA) [3]), as shown in Tab. 8. Note that AdvLoRA is adapted under PGD-3. The experimental results indicate that (1) AdvLoRA consistently outperforms the baseline model, LoRA, across various attack types. This trend continues with the FGSM attack, where AdvLoRA scores 84.44 and 72.21, compared to LoRA's 61.01 and

54.41. (2) AdvLoRA also demonstrates strong performance under black-box attacks. For the SA, AdvLoRA attains a TR mean score of 87.40 and an IR mean score of 75.83, highlighting its robustness against unseen attack strategies. The results collectively affirm that AdvLoRA not only enhances robustness through adversarial adaptation but also generalizes effectively across different attack types, thereby reinforcing the model's applicability in real-world scenarios where diverse adversarial threats may be encountered.

Scaling to Larger Backbones. To demonstrate the scalability of the proposed method, we evaluated various sizes of BLIP as the backbone on Flickr30K, as shown in Tab. 9. The findings indicate that: (1) *Consistent Performance Improvement.* AdvLoRA consistently outperforms the baseline model, LoRA, across both TR and IR metrics, achieving notable scores for different backbone sizes. (2) *Enhanced Capability Utilization.* This trend continues with the larger BLIP architectures, where AdvLoRA maintains a clear performance edge over LoRA. (3) *Significant Gains in Larger Architectures.* When scaling to the larger BLIP-2-opt-2.7b backbone, AdvLoRA shows substantial improvements, reaffirming its effectiveness. These results highlight AdvLoRA's robustness and adaptability, confirming its ability to leverage larger architectures for enhanced retrieval performance. This scalability not only improves model efficiency but also supports its application in complex real-world scenarios, where capturing intricate data patterns is crucial.

Table 9: Performance on Flickr30K when scaling to larger backbone networks. "TR" and "IR" donate text-to-image retrieval and image-to-text retrieval.

Backbone	Method	TR@Mean	IR@Mean	Mean
BLIP-base	LoRA	80.40	73.24	76.82
	AdvLoRA	82.83	74.67	78.75
BLIP-large	LoRA	81.73	73.01	77.34
	AdvLoRA	84.74	75.56	80.15
BLIP-2-opt-2.7b	LoRA	83.32	81.18	82.25
	AdvLoRA	87.34	83.66	85.50

Table 10: Performance on Flickr30K when scaling to larger backbone networks. "TR" and "IR" donate text-to-image retrieval and image-to-text retrieval.

| Method	TR@Mean	IR@Mean	R@Mean
BLIP+FFT*+Nat.	74.17	69.11	71.65
BLIP+LoRA*+Nat.	85.29	74.75	80.02
BLIP+LP*+Nat.	86.33	75.38	80.86
UniAdapter*+Nat.	75.29	66.89	71.09
Aurora*+Nat.	84.74	73.54	79.15
AdvLoRA*+Nat.	85.18	74.67	79.92

Performance on the Natural Data. To evaluate the performance of our proposed method on natural images, we assess AdvLoRA and five baselines on MSCOCO, as shown in Tab. 10. The findings indicate: (1) *Trade-off in Performance.* While adversarial adaptation enhances robustness against specific attacks, it can degrade performance on natural data, suggesting a trade-off between adversarial resilience and generalization. (2) *Superior Metrics of AdvLoRA.* AdvLoRA achieves a TR mean score of 85.18 and an IR mean score of 79.92, surpassing all baselines due to its ability to learn semantically invariant feature representations. (3) *Versatility Across Retrieval Tasks.* Compared to methods like BLIP+FFT and UniAdapter, AdvLoRA excels in TR and IR metrics, demonstrating a retrieval mean score of 79.92, underscoring its reliability. These results affirm AdvLoRA's effectiveness in balancing robustness and performance in natural image retrieval.

Case Study. To visually demonstrate the effectiveness of AdvLoRA, we present several test cases from the MSR-VTT dataset, as illustrated in Fig. 5. The results show that: (1) *Resilience to Adversarial Attacks.* In Video168, AdvLoRA retrieves "He is playing with ball," accurately reflecting the scene despite adversarial perturbations, while Aurora shows a noticeable decline in performance. (2) *Contextual Understanding.* For Video8915, AdvLoRA identifies "Women preparing to cook a roast," demonstrating its ability to grasp contextual details, whereas Aurora's output lacks the same level of accuracy. (3) *Complex Scene Interpretation.* In Video128, AdvLoRA maintains clarity in retrieving a cartoon character preparing to ride a bicycle, contrasting with Aurora's irrelevant result, highlighting AdvLoRA's ability to retain semantic integrity amid adversarial challenges. These examples underscore AdvLoRA's robustness and contextual awareness in dynamic environments.

Video7168:
AdvLoRA retrieval result: He is playing with ball
Aurora retrieval result: Some people video conferencing as they watch a movie
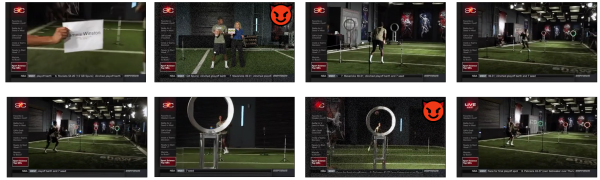
Video8915:
AdvLoRA retrieval result: Person cooking up somefood
Aurora retrieval result: A women preparing a duck to roast

Video8128:
AdvLoRA retrieval result: A cartoon character prepares to ride a bicycle
Aurora retrieval result: People are walking down a street holding signs

Figure 5: Case study of MSR-VTT. We sample and visualize eight frames from the videos. The frames with the devil denote that they are under the adversarial attacks.

5 CONCLUSION

In this paper, we aim to alleviate the security risks in the Vision-Language Models (VLMs). First of all, we show the vulnerability of VLMs with various adaptation methods under adversarial attacks via extensive experiments. Besides, as the sizes of VLMs increase, simply applying the conventional adversarial adaptation methods to VLMs easily leads to (1) unpromising adversarial robustness and (2) tremendous parameter costs. To tackle these issues, we propose a novel parameter-efficient adversarial adaptation method called AdvLoRA, which incorporates parameter clustering, parameter alignment, and adaptive parameter updates. Extensive experiments validate the effectiveness and efficiency of AdvLoRA, revealing the intrinsic low-rank property that emerges during the adversarial adaptation process. Our technique, which emphasizes clustering reparameterization and parameter alignment, significantly enhances the adaptation process. This work provides a fresh perspective for researchers focused on security within the broader context of Artificial General Intelligence (AGI). Moving forward, we aim to optimize memory and computational resources during the adaptation process and enhance the adversarial robustness of VLMs, particularly against language-based attacks.

REFERENCES

[1] Josh Achiam, Steven Adler, Sandhini Agarwal, Lama Ahmad, Ilge Akkaya, Florencia Leoni Aleman, Diogo Almeida, Janko Altenschmidt, Sam Altman, Shyamal Anadkat, et al. 2023. Gpt-4 technical report. *arXiv preprint arXiv:2303.08774* (2023).

[2] Zeyuan Allen-Zhu and Yuanzhi Li. 2022. Feature purification: How adversarial training performs robust deep learning. In *FOCS*. IEEE, 977–988.

[3] Maksym Andriushchenko, Francesco Croce, Nicolas Flammarion, and Matthias Hein. 2020. Square attack: a query-efficient black-box adversarial attack via random search. In *ECCV*. Springer, 484–501.

[4] Lisa Anne Hendricks, Oliver Wang, Eli Shechtman, Josef Sivic, Trevor Darrell, and Bryan Russell. 2017. Localizing moments in video with natural language. In *ICCV*. 5803–5812.

[5] Hyojin Bahng, Ali Jahanian, Swami Sankaranarayanan, and Phillip Isola. 2022. Exploring visual prompts for adapting large-scale models. *arXiv preprint arXiv:2203.17274* (2022).

[6] Max Bain, Arsha Nagrani, Gül Varol, and Andrew Zisserman. 2021. Frozen in time: A joint video and image encoder for end-to-end retrieval. In *ICCV*. 1728–1738.

[7] Fan Bao, Shen Nie, Kaiwen Xue, Chongxuan Li, Shi Pu, Yaole Wang, Gang Yue, Yue Cao, Hang Su, and Jun Zhu. 2023. One transformer fits all distributions in multi-modal diffusion at scale. *arXiv preprint arXiv:2303.06555* (2023).

[8] Yichao Cai, Yuhang Liu, Zhen Zhang, and Javen Qinfeng Shi. 2023. CLAP: Contrastive Learning with Augmented Prompts for Robustness on Pretrained Vision-Language Models. *arXiv preprint arXiv:2311.16445* (2023).

[9] Pin-Yu Chen, Huan Zhang, Yash Sharma, Jinfeng Yi, and Cho-Jui Hsieh. 2017. Zoo: Zeroth order optimization based black-box attacks to deep neural networks without training substitute models. In *Proceedings of the 10th ACM workshop on artificial intelligence and security*. 15–26.

[10] Tim Dettmers, Artidoro Pagnoni, Ari Holtzman, and Luke Zettlemoyer. 2023. Qlora: Efficient finetuning of quantized llms. *arXiv preprint arXiv:2305.14314* (2023).

[11] Yunfeng Diao, Baiqi Wu, Ruixuan Zhang, Ajian Liu, Xingxing Wei, Meng Wang, and He Wang. 2024. TASAR: Transfer-based Attack on Skeletal Action Recognition. *arXiv preprint arXiv:2409.02483* (2024).

[12] Nanyi Fei, Zhiwu Lu, Yizhao Gao, Guoxing Yang, Yuqi Huo, Jingyuan Wen, Haoyu Lu, Ruihua Song, Xin Gao, Tao Xiang, et al. 2022. Towards artificial general intelligence via a multimodal foundation model. *Nature Communications* (2022), 3094.

[13] Shuo Feng, Xintao Yan, Haowei Sun, Yiheng Feng, and Henry X Liu. 2021. Intelligent driving intelligence test for autonomous vehicles with naturalistic and adversarial environment. *Nature communications* (2021), 748.

[14] Samuel G Finlayson, John D Bowers, Joichi Ito, Jonathan L Zittrain, Andrew L Beam, and Isaac S Kohane. 2019. Adversarial attacks on medical machine learning. *Science* (2019), 1287–1289.

[15] Zhe Gan, Yen-Chun Chen, Linjie Li, Chen Zhu, Yu Cheng, and Jingjing Liu. 2020. Large-scale adversarial training for vision-and-language representation learning. *NeurIPS* (2020), 6616–6628.

[16] Peng Gao, Shijie Geng, Renrui Zhang, Teli Ma, Rongyao Fang, Yongfeng Zhang, Hongsheng Li, and Yu Qiao. 2023. Clip-adapter: Better vision-language models with feature adapters. *International Journal of Computer Vision* (2023), 581–595.

[17] Ben Goertzel. 2014. Artificial general intelligence: concept, state of the art, and future prospects. *Journal of Artificial General Intelligence* (2014), 1.

[18] Ian J Goodfellow, Jonathon Shlens, and Christian Szegedy. 2014. Explaining and harnessing adversarial examples. *arXiv preprint arXiv:1412.6572* (2014).

[19] Xiaoshuai Hao and Wanqian Zhang. 2024. Uncertainty-aware alignment network for cross-domain video-text retrieval. *NeurIPS* (2024).

[20] Xiaoshuai Hao, Wanqian Zhang, Dayan Wu, Fei Zhu, and Bo Li. 2022. Listen and look: Multi-modal aggregation and co-attention network for video-audio retrieval. In *ICME*. 1–6.

[21] Xiaoshuai Hao, Wanqian Zhang, Dayan Wu, Fei Zhu, and Bo Li. 2023. Dual alignment unsupervised domain adaptation for video-text retrieval. In *CVPR*. 18962–18972.

[22] Xiaoshuai Hao, Yucan Zhou, Dayan Wu, Wanqian Zhang, Bo Li, and Weiping Wang. 2021. Multi-feature graph attention network for cross-modal video-text retrieval. In *ICMR*. 135–143.

[23] Xiaoshuai Hao, Yucan Zhou, Dayan Wu, Wanqian Zhang, Bo Li, Weiping Wang, and Dan Meng. 2021. What matters: Attentive and relational feature aggregation network for video-text retrieval. In *ICME*. 1–6.

[24] Xiaoshuai Hao, Yi Zhu, Srikar Appalaraju, Aston Zhang, Wanqian Zhang, Bo Li, and Mu Li. 2023. Mixgen: A new multi-modal data augmentation. In *WACV*. 379–389.

[25] Edward J Hu, Yelong Shen, Phillip Wallis, Zeyuan Allen-Zhu, Yuanzhi Li, Shean Wang, Lu Wang, and Weizhu Chen. 2021. Lora: Low-rank adaptation of large language models. *arXiv preprint arXiv:2106.09685* (2021).

[26] Menglin Jia, Luming Tang, Bor-Chun Chen, Claire Cardie, Serge Belongie, Bharath Hariharan, and Ser-Nam Lim. 2022. Visual prompt tuning. In *ECCV*. 709–727.

[27] Alexey Kurakin, Ian Goodfellow, and Samy Bengio. 2016. Adversarial machine learning at scale. *arXiv preprint arXiv:1611.01236* (2016).

[28] Junnan Li, Dongxu Li, Caiming Xiong, and Steven Hoi. 2022. Blip: Bootstrapping language-image pre-training for unified vision-language understanding and generation. In *ICML*. 12888–12900.

[29] Tsung-Yi Lin, Michael Maire, Serge Belongie, James Hays, Pietro Perona, Deva Ramanan, Piotr Dollár, and C Lawrence Zitnick. 2014. Microsoft coco: Common objects in context. In *ECCV*. 740–755.

[30] Ninghao Liu, Hongxia Yang, and Xia Hu. 2018. Adversarial detection with model interpretation. In *KDD*. 1803–1811.

[31] Xiaodong Liu, Hao Cheng, Pengcheng He, Weizhu Chen, Yu Wang, Hoifung Poon, and Jianfeng Gao. 2020. Adversarial training for large neural language models. *arXiv preprint arXiv:2004.08994* (2020).

[32] Xiao Liu, Yanan Zheng, Zhengxiao Du, Ming Ding, Yujie Qian, Zhilin Yang, and Jie Tang. 2023. GPT understands, too. *AI Open* (2023), 208–215.

[33] Yue Liu, Hongcheng Gao, Shengfang Zhai, Jun Xia, Tianyi Wu, Zhiwei Xue, Yulin Chen, Kenji Kawaguchi, Jiaheng Zhang, and Bryan Hooi. 2025. GuardReasoner: Towards Reasoning-based LLM Safeguards. *arXiv preprint arXiv:2501.18492* (2025).

[34] Yue Liu, Xiaoxin He, Miao Xiong, Jinlan Fu, Shumin Deng, and Bryan Hooi. 2024. Flipattack: Jailbreak llms via flipping. *arXiv preprint arXiv:2410.02832* (2024).

[35] Zeyu Liu, Souvik Kundu, Anni Li, Junrui Wan, Lianghao Jiang, and Peter Anthony Beerel. 2024. AFLoRA: Adaptive Freezing of Low Rank Adaptation in Parameter Efficient Fine-Tuning of Large Models. *arXiv preprint arXiv:2403.13269* (2024).

[36] Haoyu Lu, Mingyu Ding, Yuqi Huo, Guoxing Yang, Zhiwu Lu, Masayoshi Tomizuka, and Wei Zhan. 2023. UniAdapter: Unified Parameter-Efficient Transfer Learning for Cross-modal Modeling. *arXiv preprint arXiv:2302.06605* (2023).

[37] Yuning Lu, Jianzhuang Liu, Yonggang Zhang, Yajing Liu, and Xinmei Tian. 2022. Prompt distribution learning. In *CVPR*. 5206–5215.

[38] Xingjun Ma, Yuhao Niu, Lin Gu, Yisen Wang, Yitian Zhao, James Bailey, and Feng Lu. 2021. Understanding adversarial attacks on deep learning based medical image analysis systems. *Pattern Recognition* (2021), 107332.

[39] Aleksander Madry. 2017. Towards deep learning models resistant to adversarial attacks. *arXiv preprint arXiv:1706.06083* (2017).

[40] Chengzhi Mao, Scott Geng, Junfeng Yang, Xin Wang, and Carl Vondrick. 2022. Understanding zero-shot adversarial robustness for large-scale models. *arXiv preprint arXiv:2212.07016* (2022).

[41] Jan Hendrik Metzen, Tim Genewein, Volker Fischer, and Bastian Bischoff. 2017. On detecting adversarial perturbations. *arXiv preprint arXiv:1702.04267* (2017).

[42] John Morris, Eli Lifland, Jin Yong Yoo, Jake Grigsby, Di Jin, and Yanjun Qi. 2020. TextAttack: A Framework for Adversarial Attacks, Data Augmentation, and Adversarial Training in NLP. In *EMNLP*. 119–126.

[43] Rui Pan, Xiang Liu, Shizhe Diao, Renjie Pi, Jipeng Zhang, Chi Han, and Tong Zhang. 2024. LISA: Layerwise Importance Sampling for Memory-Efficient Large Language Model Fine-Tuning. *arXiv preprint arXiv:2403.17919* (2024).

[44] Tianyu Pang, Xiao Yang, Yinpeng Dong, Hang Su, and Jun Zhu. 2020. Bag of tricks for adversarial training. *arXiv preprint arXiv:2010.00467* (2020).

[45] Jing Pei, Lei Deng, Sen Song, Mingguo Zhao, Youhui Zhang, Shuang Wu, Guanrui Wang, Zhe Zou, Zhenzhi Wu, Wei He, et al. 2019. Towards artificial general intelligence with hybrid Tianjic chip architecture. *Nature* (2019), 106–111.

[46] Bryan A Plummer, Liwei Wang, Chris M Cervantes, Juan C Caicedo, Julia Hockenmaier, and Svetlana Lazebnik. 2015. Flickr30k entities: Collecting region-to-phrase correspondences for richer image-to-sentence models. In *ICCV*. 2641–2649.

[47] Rushi Qiang, Ruiyi Zhang, and Pengtao Xie. 2024. BiLoRA: A Bi-level Optimization Framework for Overfitting-Resilient Low-Rank Adaptation of Large Pre-trained Models. *arXiv preprint arXiv:2403.13037* (2024).

[48] Robin Rombach, Andreas Blattmann, Dominik Lorenz, Patrick Esser, and Björn Ommer. 2022. High-resolution image synthesis with latent diffusion models. In *CVPR*. 10684–10695.

[49] Mahmood Sharif, Sruti Bhagavatula, Lujo Bauer, and Michael K Reiter. 2016. Accessorize to a crime: Real and stealthy attacks on state-of-the-art face recognition. In *Proceedings of the 2016 acm sigsac conference on computer and communications security*. 1528–1540.

[50] Christian Szegedy, Wojciech Zaremba, Ilya Sutskever, Joan Bruna, Dumitru Erhan, Ian Goodfellow, and Rob Fergus. 2013. Intriguing properties of neural networks. *arXiv preprint arXiv:1312.6199* (2013).

[51] Rajagopal Venkatesaramani, Bradley A Malin, and Yevgeniy Vorobeychik. 2021. Re-identification of individuals in genomic datasets using public face images. *Science advances* (2021), eabg3296.

[52] Riccardo Volpi, Hongseok Namkoong, Ozan Sener, John C Duchi, Vittorio Murino, and Silvio Savarese. 2018. Generalizing to unseen domains via adversarial data augmentation. *NeurIPS* (2018), 5339–5349.

[53] Haixin Wang, Xinlong Yang, Jianlong Chang, Dian Jin, Jinan Sun, Shikun Zhang, Xiao Luo, and Qi Tian. 2023. Parameter-efficient Tuning of Large-scale Multimodal Foundation Model. In *NeurIPS*. 15752–15774.

[54] Sheng Wang, Liheng Chen, Jiyue Jiang, Boyang Xue, Lingpeng Kong, and Chuan Wu. 2024. LoRA Meets Dropout under a Unified Framework. *arXiv preprint arXiv:2403.00812* (2024).

[55] Yu-Xiong Wang, Deva Ramanan, and Martial Hebert. 2017. Growing a brain: Fine-tuning by increasing model capacity. In *CVPR*. 2471–2480.

[56] Xingxing Wei, Jun Zhu, Sha Yuan, and Hang Su. 2019. Sparse adversarial perturbations for videos. In *AAAI*. 8973–8980.

[57] Mitchell Wortsman, Gabriel Ilharco, Jong Wook Kim, Mike Li, Simon Kornblith, Rebecca Roelofs, Raphael Gontijo Lopes, Hannaneh Hajishirzi, Ali Farhadi, Hongseok Namkoong, et al. 2022. Robust fine-tuning of zero-shot models. In *CVPR*. 7959–7971.

[58] Wenhao Wu, Zhun Sun, and Wanli Ouyang. 2022. Transferring textual knowledge for visual recognition. *arXiv preprint arXiv:2207.01297* (2022).

[59] Yinghui Xing, Qirui Wu, De Cheng, Shizhou Zhang, Guoqiang Liang, and Yanning Zhang. 2022. Class-aware visual prompt tuning for vision-language pre-trained model. *arXiv preprint arXiv:2208.08340* (2022).

[60] Jun Xu, Tao Mei, Ting Yao, and Yong Rui. 2016. Msr-vtt: A large video description dataset for bridging video and language. In *CVPR*. 5288–5296.

[61] Xilie Xu, Jingfeng Zhang, and Mohan Kankanhalli. [n. d.]. AutoLoRa: An Automated Robust Fine-Tuning Framework. In *The Twelfth International Conference on Learning Representations*.

[62] Zheng Yuan, Jie Zhang, and Shiguang Shan. 2024. Fulllora-at: Efficiently boosting the robustness of pretrained vision transformers. *arXiv preprint arXiv:2401.01752* (2024).

[63] Haotian Zhang, Pengchuan Zhang, Xiaowei Hu, Yen-Chun Chen, Liunian Li, Xiyang Dai, Lijuan Wang, Lu Yuan, Jenq-Neng Hwang, and Jianfeng Gao. 2022. Glipv2: Unifying localization and vision-language understanding. *NeurIPS* (2022), 36067–36080.

[64] Jiaming Zhang, Xingjun Ma, Xin Wang, Lingyu Qiu, Jiaqi Wang, Yu-Gang Jiang, and Jitao Sang. 2023. Adversarial prompt tuning for vision-language models. *arXiv preprint arXiv:2311.11261* (2023).

[65] Qingru Zhang, Minshuo Chen, Alexander Bukharin, Pengcheng He, Yu Cheng, Weizhu Chen, and Tuo Zhao. 2023. Adaptive budget allocation for parameter-efficient fine-tuning. *arXiv preprint arXiv:2303.10512* (2023).

[66] Qingzhao Zhang, Shengtuo Hu, Jiachen Sun, Qi Alfred Chen, and Z Morley Mao. 2022. On adversarial robustness of trajectory prediction for autonomous vehicles. In *CVPR*. 15159–15168.

[67] Jiawei Zhao, Zhenyu Zhang, Beidi Chen, Zhangyang Wang, Anima Anandkumar, and Yuandong Tian. 2024. Galore: Memory-efficient llm training by gradient low-rank projection. *arXiv preprint arXiv:2403.03507* (2024).

[68] Yunqing Zhao, Tianyu Pang, Chao Du, Xiao Yang, Chongxuan Li, Ngai-Man Cheung, and Min Lin. 2023. On evaluating adversarial robustness of large vision-language models. *arXiv preprint arXiv:2305.16934* (2023).

[69] Ming Zhong, Yelong Shen, Shuohang Wang, Yadong Lu, Yizhu Jiao, Siru Ouyang, Donghan Yu, Jiawei Han, and Weizhu Chen. 2024. Multi-LoRA Composition for Image Generation. *arXiv preprint arXiv:2402.16843* (2024).

[70] Kaiyang Zhou, Jingkang Yang, Chen Change Loy, and Ziwei Liu. 2022. Learning to prompt for vision-language models. *International Journal of Computer Vision* (2022), 2337–2348.